Am J Transl Res 2025;17(11):8567-8576
www.ajtr.org /ISSN:1943-8141/AJTR0165792

Original Article

Urinary exosomal miR-320b as a biomarker of tubular atrophy/interstitial fibrosis in IgA nephropathy patients

Yiqi Huang[1], Zhongjie Qu[2], Yanling Zhang[1], Feng Jin[1], Jiahua Jin[3]

[1]Department of Nephrology, Shaoxing Second Hospital, Shaoxing, Zhejiang, China; [2]Department of Nephrology, The Third Affiliated Hospital of Zhejiang Chinese Medical University (Zhongshan Hospital of Zhejiang Province), Hangzhou, Zhejiang, China; [3]Department of Ultrasound, Shaoxing Second Hospital, Shaoxing, Zhejiang, China

Received May 3, 2025; Accepted October 28, 2025; Epub November 15, 2025; Published November 30, 2025

Abstract: Objective: Tubular atrophy/interstitial fibrosis (TA/IF) is an independent risk factor for the progression of immunoglobulin A nephropathy (IgAN), with its assessment primarily relying on renal biopsy. Therefore, this study aimed to identify novel non-invasive biomarkers for the dynamic evaluation of TA/IF in IgAN patients. Methods: IgAN patients were divided into T0 (TA/IF ≤ 25%) and T1 (TA/IF > 25%) groups. Urine exosomes were isolated from morning samples by ultracentrifugation and characterized using electron microscopy, nanoparticle tracking, and western blot. High-throughput sequencing, real-time quantitative polymerase chain reaction (RT-qPCR), and receiver operating characteristic curve (ROC) analysis identified microRNA-320b (miR-320b) as the best candidate for predicting TA/IF scores in IgAN. Hence, the association between miR-320b expression and clinical data was evaluated. Results: Compared to the T0 group, significantly higher blood urea nitrogen (BUN), serum creatinine (Scr), uric acid (UA), and 24-hour urine protein quantification (24UP) levels were observed in the T1 group. In contrast, hemoglobin (Hb), albumin (Alb), and estimated glomerular filtration rate (eGFR) were lower ($P < 0.05$). In the T1 group, 9 miRNAs were upregulated and 16 were downregulated. RT-qPCR analysis revealed that these 9 miRNAs were significantly overexpressed in the T1 group ($P < 0.05$), with miR-320b showing the most significant upregulation ($P < 0.001$). In addition, ROC curve analysis indicated that miR-320b had good diagnostic efficacy (AUC = 0.8785, P = 0.0017). Spearman correlation analysis revealed that miR-320b expression was positively linked to 24UP, BUN, Scr, and UA, and negatively linked to eGFR. Conclusion: Urine exosomal miR-320b is a non-invasive biomarker that can effectively predict TA/IF scores in IgAN patients, offering a promising alternative for diagnosing renal fibrosis in this population.

Keywords: Tubular atrophy/interstitial fibrosis, immunoglobulin a nephropathy, exosomal, miR-320b, epithelial-mesenchymal transition

Introduction

Immunoglobulin A nephropathy (IgAN) is the most prevalent primary glomerulonephritis [1], with an incidence ranging from 10% in European and American countries to 50% in Asian regions [2, 3]. Approximately 20-40% of IgAN patients progress to end-stage renal disease (ESRD) within 10-20 years after diagnosis [4-6]. Research shows that all pathologic indicators of the Oxford classification are closely related to the progression of IgAN [7]. Among them, tubular atrophy/interstitial fibrosis (TA/IF) is an independent risk factor for disease progression and the strongest predictor of renal survival [8, 9]. Currently, the TA/IF score is determined primarily by renal biopsy. However, renal tissue biopsy involves complications such as bleeding and infection, and many patients cannot undergo repeated biopsies due to contraindications. Therefore, a non-invasive biomarker that can dynamically assess the TA/IF score of IgAN patients is needed.

Exosomes are small vesicles with a diameter of 30-150 nm secreted by living cells, and are widely found in body fluids such as blood, urine, and saliva [10, 11]. These carry various bioactive molecules, including proteins, messenger RNA (mRNA), and microRNA (miRNA), and participate in intercellular material and signal transmission, thereby regulating pathophysio-

https://doi.org/10.62347/MDEV3576

logic processes [11]. miRNA is an endogenous non-coding small RNA molecule. By specifically binding to target mRNA, miRNAs regulate gene expression and participate in biological processes such as cell proliferation, differentiation, apoptosis, and fibrosis [12]. In recent years, miRNAs derived from urinary exosomes have emerged as an ideal source for biomarkers of kidney diseases due to their non-invasive nature, stability, and ease of acquisition [13]. Studies have shown that miRNAs in urinary exosomes are differentially expressed in various kidney diseases and may be involved in the progression of renal fibrosis [14]. Therefore, this study aims to identify non-invasive biomarkers for predicting the TA/IF score in IgAN patients.

Patients and methods

Subjects

Patients diagnosed with IgAN by renal biopsy at Shaoxing Second Hospital from January 2020 to December 2022 were retrospectively screened. The included patients were divided into two groups based on the Oxford classification TA/IF score, namely the T0 group (TA/IF ≤ 25%) and the T1 group (TA/IF > 25%). The exclusion criteria included malignant tumors, lupus, acute infections, significant fibrosis in organs other than the kidneys, use of glucocorticoids or immunosuppressants for over 3 months, and prior kidney transplantation. Basic patient information was collected, including age, gender, albumin (Alb), serum creatinine (Scr), uric acid (UA), estimated glomerular filtration rate (eGFR), and 24-hour urine protein quantification (24UP). All participants provided informed consent, and the study was approved by the Ethics Committee of Shaoxing Second Hospital.

Sample processing and exosome extraction

Morning urine samples from patients with IgAN were collected. The urine samples were centrifuged at 2000 × g for 30 min at 4°C within 2 hours after collection. The supernatant was transferred to a new centrifuge tube and centrifuged again at 10,000 × g for 45 min at 4°C to remove larger vesicles. The supernatant was filtered through a 0.45 μm filter, and the filtrate was collected. An ultracentrifuge rotor was used, and the sample was centrifuged at 100,000 × g for 70 min at 4°C. The supernatant was removed, and the pellet was resuspended in 10 mL of pre-cooled phosphate-buffered saline (PBS). Subsequently, the sample was centrifuged again at 100,000 × g for 70 min at 4°C. Finally, the supernatant was removed, and the exosome pellet was resuspended in PBS and stored at -80°C for future use.

Observation by transmission electron microscopy (TEM)

Specifically, 10 μL of exosome sample was placed onto a copper grid for 1 min to allow precipitation. Filter paper was used to remove the supernatant. Then, 10 μL of acetate uranyl was added and allowed to precipitate on the copper grid for 1 min. Again, filter paper was used to remove the supernatant. The samples were allowed to dry at room temperature for several minutes and then subjected to TEM imaging (HT-7700, Hitachi) at 80 kV.

Particle size analysis

In this experiment, 10 μL of the exosome sample was diluted to 30 μL with PBS. The instrument performance was tested based on the standard sample, and the exosome sample was loaded. Following sample detection, the particle size and concentration information of the exosomes were measured by the nanoparticle size analyzer (N30E, NanoFCM).

Western blotting

Exosomes or human kidney-2 (HK-2) cells were thawed at 37°C and then lysed with radioimmunoprecipitation assay buffer lysis buffer on ice for 30 minutes. The protein concentration was determined by the BCA method. The proteins were separated by 12% sodium dodecyl sulfate-polyacrylamide gel electrophoresis and transferred to polyvinylidene fluoride membranes. The membranes were blocked with 5% skim milk tris-buffered saline with tween (TBST) for 1 hour, and then incubated with primary antibodies at 4°C overnight. The membranes were washed with TBST three times (10 minutes each time), and then incubated with HRP-conjugated goat anti-rabbit immunoglobulin G secondary antibody (1:5000; SA00001-2, Proteintech, China) at room temperature for 1 hour. The membranes were washed with TBST three times (10 minutes each time), and the target proteins were detected using a chemiluminescence imaging system.

Construction of exosomal miRNA libraries

Total RNA was extracted from exosomes using the miRNeasy Mini Kit (Qiagen, 217004). A miRNA library was constructed using 3 ng of RNA with the small RNA library preparation kit (KAITAI-Bio, AT4208). Thereafter, the library was sequenced on the Illumina NovaSeq 6000 platform. Sequencing and data analysis were performed by Hangzhou KAITAI Biotechnology Co., Ltd.

Analysis of exosomal miRNA sequencing data

The raw data was subjected to quality control using fastp (v0.23.0, https://github.com/OpenGene/fastp). Low-quality sequences were removed, and reads of 18-36 bp in length were retained (--length_required 18-36bp). The reference genome and gene annotation files (Homo sapiens, Ensembl v101) were downloaded from the Ensembl database. Clean data was aligned to the reference genome using HISAT2 (v2.2.1, http://daehwankimlab.github.io/hisat2/), followed by annotation using ncRNA, mRNA, and miRNA databases to calculate the proportion of various RNAs (miRNA, tRNA, rRNA, snRNA, and mRNA). Novel miRNAs were predicted based on miRDeep2 (https://www.mdc-berlin.de/8551903/en/), and miRNA expression levels and RPM values were calculated using a custom script. Differential expression analysis was performed using edgeR (https://bioconductor.org/packages/release/bioc/html/edgeR.html), with significance thresholds set at FDR < 0.05 and |log2FC| > 1. The target genes of differentially expressed miRNAs were predicted using miRanda and TargetScan, and the genes predicted by both methods were selected as the final target genes. To determine the biological functions and related pathways of the target genes, Gene Ontology (GO) (http://geneontology.org/) and Kyoto Encyclopedia of Genes and Genomes (KEGG) (http://www.kegg.jp/) enrichment analyses were conducted with a significance threshold of $P < 0.05$.

Reverse transcription and quantitative real-time polymerase chain reaction (RT-qPCR) analysis miRNA was extracted from cells/tissues using the miRNA extraction kit (RC201, Vazyme) according to the manufacturer's instructions. Subsequently, reverse transcription was performed using the miRNA tailing reverse transcription kit (MR201-01, Vazyme). Quantitative real-time PCR was carried out on the ABI Quant Studio Sequence Detection System (Applied Biosystems, Foster City, CA, USA), and the reaction system used the highly specific miRNA dye qPCR Mix (MQ102-01, Vazyme).

Statistical analysis

Statistical analysis and graphing were performed using SPSS 22.0 (IBM, USA) and Prism 8.0.1 (GraphPad, USA). The measured data were expressed as mean ± SD, and the t-test was carried out to compare the results of various groups. The counted data were presented as frequency and constituent ratio, and Fisher's exact test was used for statistical analysis. Enriched GO terms and KEGG pathways were visualized using RStudio, and GO analysis networks were constructed using the Bingo plugin in Cytoscape. The diagnostic value of urinary exosomal miRNAs was evaluated by receiver operating characteristic curves (ROC), and Spearman's rank correlation analysis was used to evaluate the correlation between exosomal miRNAs and clinical data.

For all tests, $P < 0.05$ was considered significant.

Results

Subject characteristics

The basic characteristics of the subjects are listed in **Table 1**. The levels of BUN, SCr, UA, and 24UP in the T1 group were significantly increased compared with the T0 group, while the Hb, Alb, and eGFR levels were decreased ($P < 0.05$).

Characterization of urine exosomes

To determine whether the precipitate isolated from urine by ultracentrifugation consisted of exosomes, TEM was performed, revealing characteristic cup-shaped vesicles with a double-layer structure (**Figure 1A**). The nanoparticle tracking analysis indicated that the particle size of the precipitate structure was approximately 80.4 nm, with a concentration of about 1.54 × 1011 particles/mL (**Figure 1B**). Western blot analysis confirmed the presence of specific surface markers of exosomes, such as cluster of differentiation 63 (CD63), cluster of differentiation 81 (CD81), and heat shock protein 70

Table 1. Clinical characteristics of the participants

Variable	Total (n = 24)	T0 (n = 12)	T1 (n = 12)	Statistic	P
Age, years	54.76 ± 3.67	54.30 ± 3.51	55.21 ± 3.93	T = -0.59	0.559
Gender, n (%)				-	1.000
Male	17 (70.83)	8 (66.67)	9 (75.00)		
Female	7 (29.17)	4 (33.33)	3 (25.00)		
Blood Urea Nitrogen, umol/L	3.65 ± 2.00	2.47 ± 1.38	4.83 ± 1.85	T = -3.54	0.002
Serum Creatinine, umol/L	116.85 ± 29.55	93.00 ± 12.10	140.71 ± 20.91	T = -6.84	< .001
Uric Acid, umol/L	435.18 ± 62.55	409.19 ± 45.97	461.17 ± 67.78	T = -2.20	0.039
Estimated Glomerular Filtration Rate, mL/min/1.73 m	78.67 ± 9.79	85.69 ± 6.78	71.65 ± 6.87	T = 5.04	< .001
24-hour Urine Protein Quantification, g	1.78 ± 0.57	1.39 ± 0.27	2.17 ± 0.53	T = -4.64	< .001
Albumin, g/L	33.54 ± 6.86	36.73 ± 6.04	30.34 ± 6.31	T = 2.53	0.019
Hemoglobin, g/L	113.02 ± 16.17	118.91 ± 15.01	107.13 ± 15.68	T = 1.88	0.044

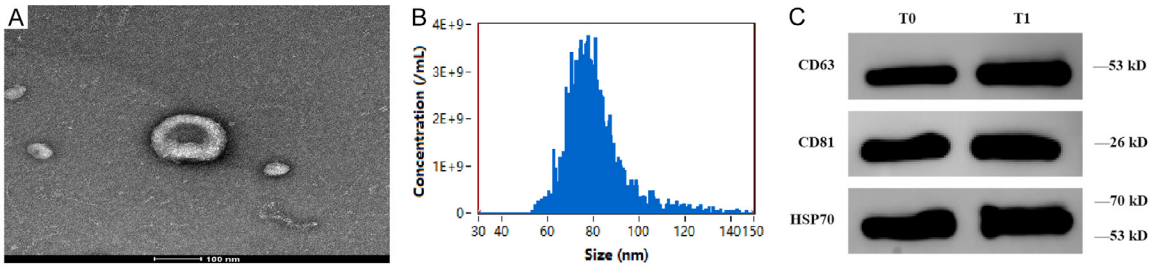

Figure 1. Characteristics of urinary exosomes in immunoglobulin A nephropathy (IgAN) patients: (A) Morphology of urinary exosomes observed by transmission electron microscopy; (B) Particle size and concentration of urinary exosomes analyzed by the nanoparticle size analyzer; (C) Specific surface markers cluster of differentiation 63 (CD63), cluster of differentiation 81 (CD81) and heat shock protein 70 (Hsp70) of urinary exosomes analyzed by western blotting.

(Hsp70) (**Figure 1C**). The original Western blot analysis of exosomal biomarkers is shown in Supplementary Figure 1. In conclusion, our experiments confirmed that the precipitate structure isolated from urine belonged to exosomes.

Screening of differentially expressed miRNAs and bioinformatic prediction

High-throughput sequencing was conducted to screen the miRNA expression profiles of exosomes in urine samples from IgAN patients in the T0 group and T1 group (**Figure 2A**). Notably, 25 differentially expressed miRNAs were identified [$p < 0.05$, log2 (fold change) > 10], among which 9 miRNAs were upregulated and 16 miRNAs were downregulated in the T1 group compared to the T0 group. **Figure 2B** displays the clustering analysis results of each differentially expressed miRNA in the samples. **Figure 2C** presents the top 10 GO terms in each GO category associated with the upregulated miRNAs. **Figure 2D** and **2E** list the important pathways identified by the KEGG and Reactome analyses of the upregulated miRNAs. The results revealed that membrane trafficking, calcium signaling pathway, Ras signaling pathway, cell adhesion molecules, focal adhesion, ErbB signaling pathway, signaling by Rho GTPases, Miro GTPases and RHOBTB3, signaling by Rho GTPases, and RAC1 GTPase cycle were all related to EMT. Therefore, subsequent experiments focused on exploring the upregulated miRNAs.

RT-qPCR validation of miRNAs

The RT-qPCR results indicated that compared to the T0 group, all 9 miRNAs in the T1 group were significantly upregulated ($P < 0.05$), among which miR-320b showed the highest degree of upregulation ($P < 0.001$) (**Figure 3**).

Diagnostic value of miRNAs for TA/IF score in patients with IgAN

The diagnostic value of urinary exosomal miRNAs for TA/IF scores in IgAN patients was determined through ROC curve analysis. The AUC and *P*-values of selected miRNAs were as fol-

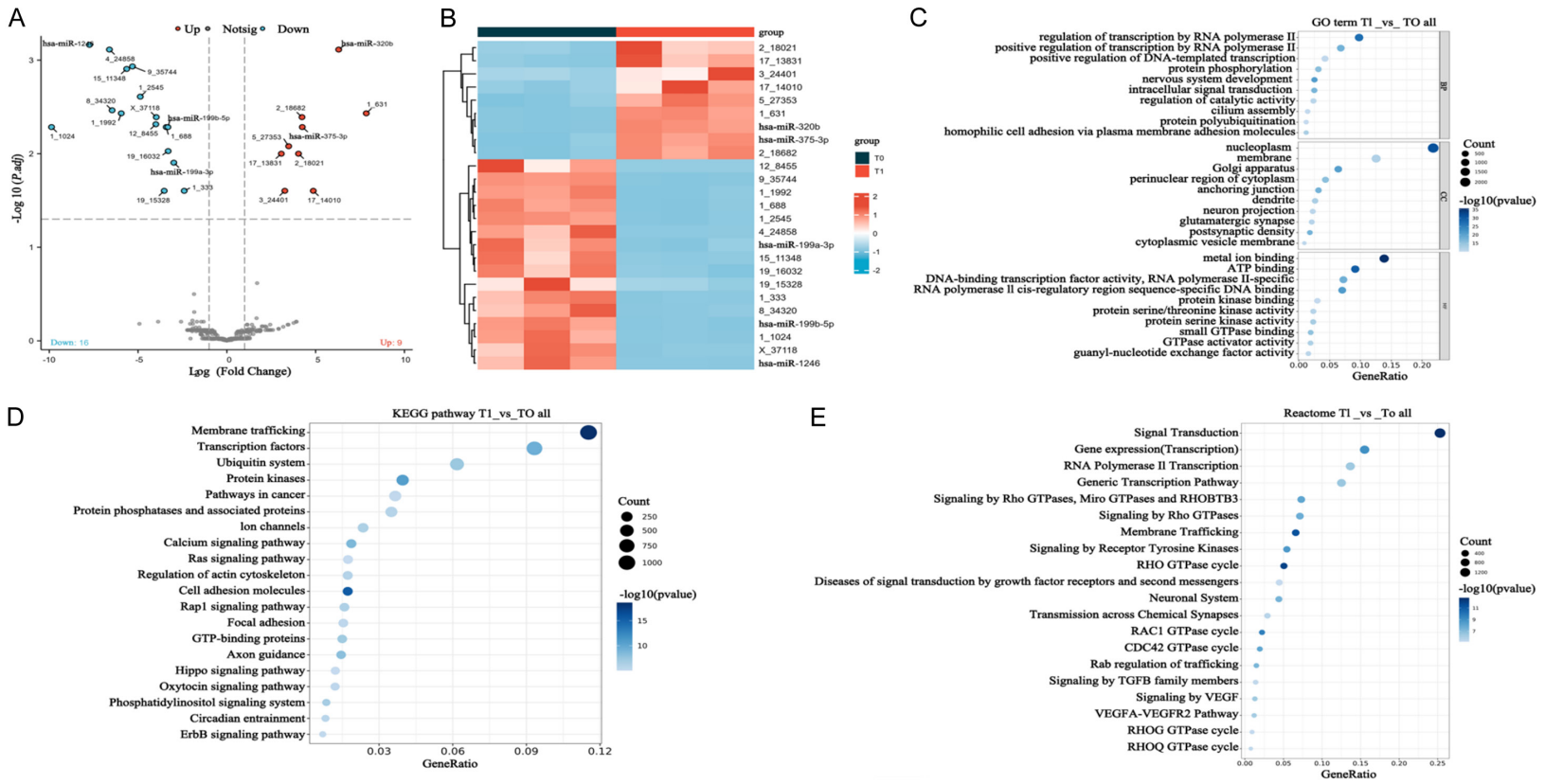

Figure 2. High-throughput sequencing and enrichment analysis: (A) Volcano plot of microRNA (miRNA) expression profiles; (B) Heatmap of miRNA expression profiles; (C) Gene Ontology (GO) analysis of upregulated miRNAs; (D) Kyoto Encyclopedia of Genes and Genomes (KEGC) analysis of upregulated miRNAs; (E) Reactome analysis of upregulated miRNAs.

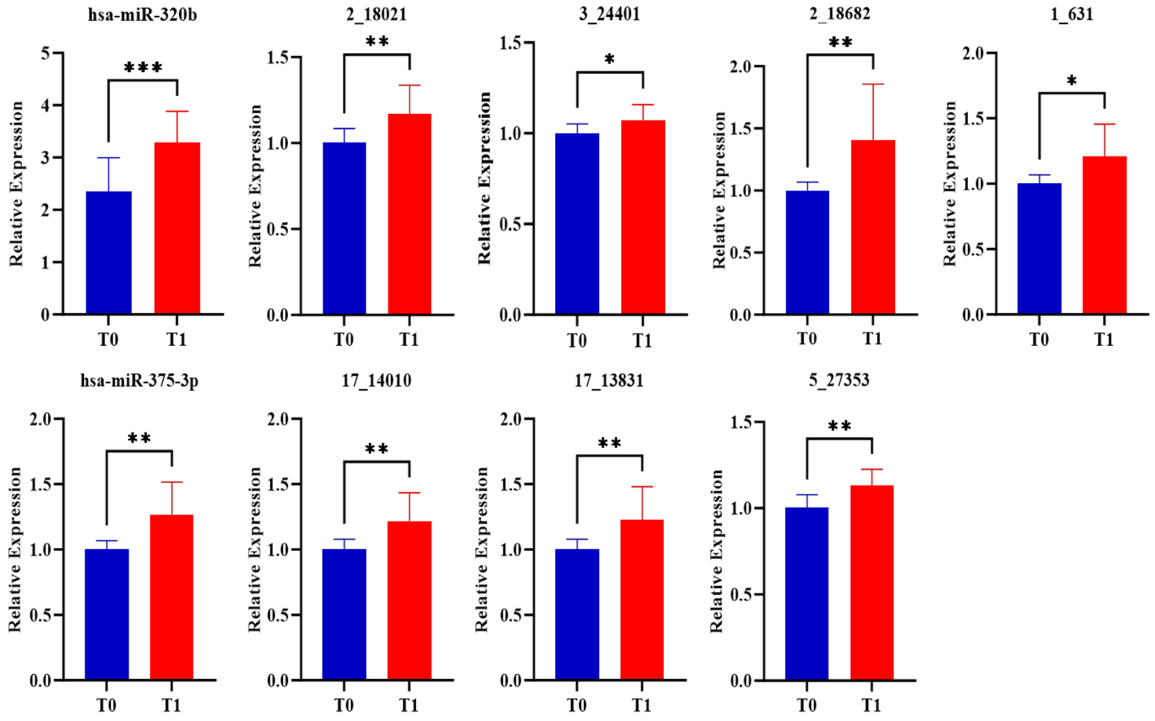

Figure 3. Comparison of urinary exosomal miRNAs levels between the T0 group and the T1 group by real-time polymerase chain reaction: * Indicates P < 0.05, ** Indicates P < 0.01, *** Indicates P < 0.001.

lows: miR-320b (AUC = 0.8785, P = 0.0017), 3_24401 (AUC = 0.7778, P = 0.0209), miR-375-3p (AUC = 0.8333, P = 0.0056), 2_18682 (AUC = 0.8264, P = 0.0067), 2_18021 (AUC = 0.8056, P = 0.0111), 17_13831 (AUC = 0.8264, P = 0.0067), 17_14010 (AUC = 0.7847, P = 0.0179), 5_27353 (AUC = 0.8472, P = 0.0039), and 1_631 (AUC = 0.7708, P = 0.0243) (**Figure 4**). Based on miRNA profiling, bioinformatic prediction, RT-qPCR, and ROC curve analysis, the role of miR-320b in tubular atrophy/interstitial fibrosis was further explored.

The correlation between miR-320b and clinical data

The expression of miR-320b was positively correlated with 24UP (r = 0.4660, P = 0.0217), BUN (r = 0.5517, P = 0.0052), SCR (r = 0.4550, P = 0.0255), and UA (r = 0.5686, P = 0.0037). In contrast, miR-320b was negatively correlated with eGFR (r = -0.5918, P = 0.0023), as shown in **Figure 5**.

Discussion

Exosome-derived miRNAs play a crucial role in intercellular material and signal transduction, participating in various biologic processes such as inflammation, cell proliferation, differentiation, and apoptosis. Consequently, they may regulate multiple pathologic processes [15]. Currently, a few studies have shown that urinary exosomal miRNAs can serve as non-invasive biomarkers for diagnosing renal fibrosis. Yua et al. detected the differential miRNAs from urinary exosomes in 38 chronic kidney disease (CKD) patients with varying degrees of renal fibrosis and 12 normal individuals [16]. The results revealed that miR-200b derived from non-proximal tubular urinary exosomes serves as a biomarker of renal fibrosis and could, to some extent, offer a non-invasive alternative to renal biopsy for assessing renal fibrosis. Epithelial-mesenchymal transition (EMT) plays a key role in renal tubulointerstitial fibrosis. Mouse experiments have confirmed that miR-30b-5p directly targets SNAI1 to regulate EMT in diabetic nephropathy [17]. These findings indicate that miR-30b-5p can not only assess the severity of renal fibrosis in DN but may also serve as a therapeutic target for improving renal fibrosis.

This study was the first to screen differential miRNAs in urinary exosomes of IgAN patients

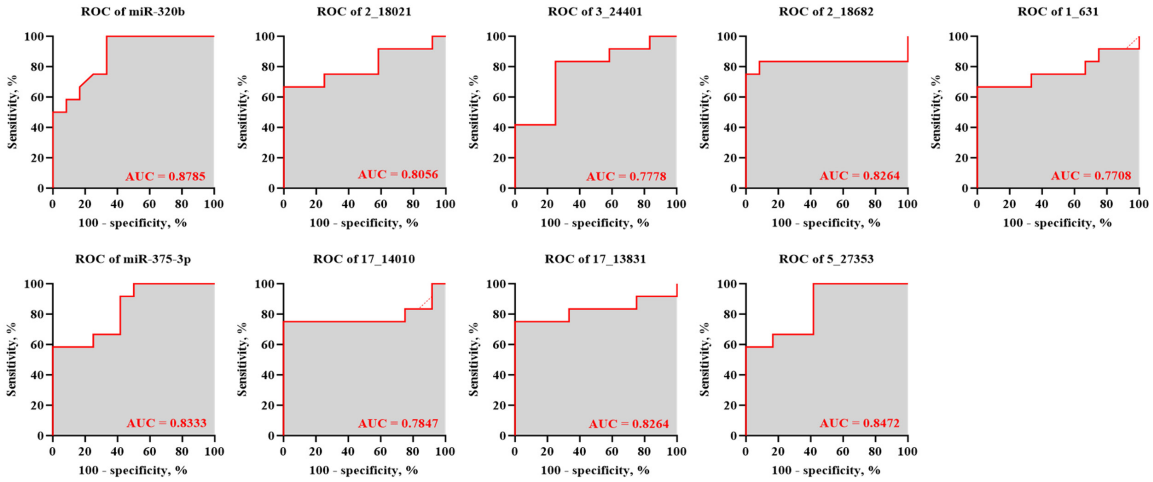

Figure 4. Evaluation of the diagnostic value of urinary exosomal miRNAs for tubular atrophy/interstitial fibrosis score in IgAN patients through receiver operating characteristic curve analysis. *Receiver Operating Characteristic Curve (ROC).

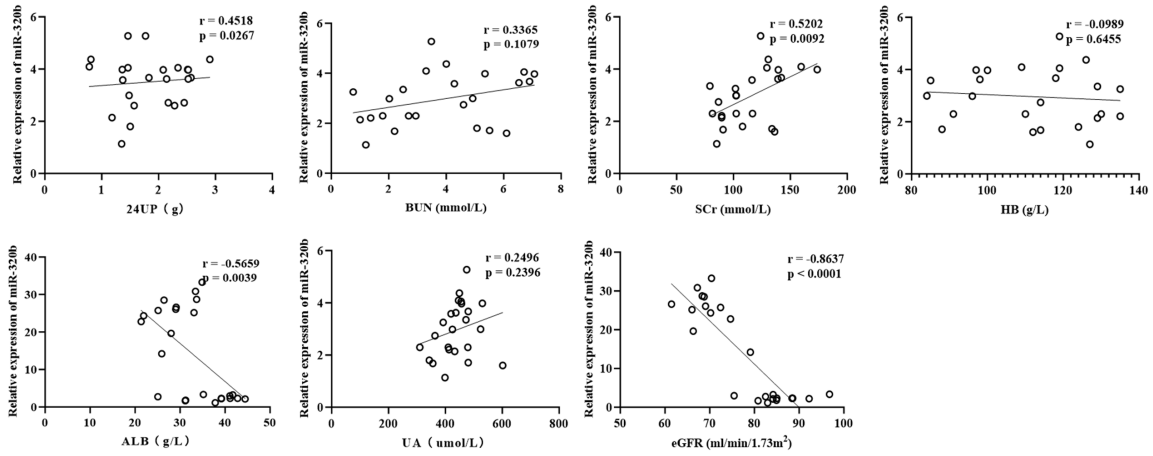

Figure 5. Correlation between the level of miR-320b in urinary exosomes of IgAN patients and clinical indicators. *24-hour Urine Protein Quantification (24UP), Blood Urea Nitrogen (BUN), Serum Creatinine (SCR), Hemoglobin (HB), Uric Acid (UA), Albumin (ALB), Estimated Glomerular Filtration Rate (eGFR).

based on the Oxford classification TA/IF score in renal biopsy. Based on the TA/IF score, IgAN patients were divided into the T0 group (TA/IF ≤ 25%) and the T1 group (TA/IF > 25%). Urine was collected, and cup-shaped vesicles were isolated by ultracentrifugation. The vesicles exhibited a size and composition consistent with that of exosomes, indicating successful extraction of exosomes. High-throughput sequencing identified 25 differentially expressed miRNAs. miRNA profiling, enrichment analysis, RT-qPCR, and ROC curve analysis identified miR-320b as the most suitable biomarker for predicting the degree of tubular atrophy/interstitial fibrosis in IgAN patients.

miR-320b is located on human chromosome 1 and belongs to the microRNA family [18]. It is an important member of the miR-320 family and plays an essential role in various biologic processes such as tumor progression, apoptosis, inflammatory states, vascular injury, and EMT [19-22]. In colorectal cancer, the upregulation of miR-320b is associated with enhanced proliferation and invasion capabilities of cancer cells [23], which might be mediated by a competitive mechanism with its homolog miRNA-320a [19]. In osteosarcoma cells, overexpression of miR-320b significantly inhibits cell viability and invasion ability while promoting apoptosis, suggesting that miR-320b may exert

its biological functions by regulating the apoptotic pathway [24]. Additionally, miR-320b participates in the proliferation and metastasis of lung cancer cells by targeting BMPR1A, highlighting its complex role in cancer [25]. In terms of inflammation and vascular injury, miR-320b can regulate the proliferation and apoptosis of scar fibroblasts by targeting β-catenin, suggesting that miR-320b effectively regulates fibrotic diseases [26]. Previous studies have reported that in the progression of esophageal squamous cell carcinoma (ESCC) [27], overexpression of miR-320b reduces the level of E-cadherin, while enhancing the expression of N-cadherin, vimentin, and Snail1. Among them, E-cadherin and N-cadherin are involved in intercellular adhesion between epithelial cells and mesenchymal cells [28, 29]. In addition, vimentin is a core component of the mesenchymal cell cytoskeleton [30], and Snail1 is a core transcription factor that induces EMT [31]. The changes in their expression are key features of the EMT process [32]. Collectively, these findings indicate that miR-320b plays a pivotal role in EMT [33, 34].

In addition, this study investigated the correlation between the expression level of miR-320b and clinical data. The results showed that compared to the T0 group, the levels of BUN, SCr, UA, Hb, Alb, and 24UP in the T1 group were significantly increased, while eGFR was decreased ($P < 0.05$). Spearman correlation analysis indicated that miR-320b was significantly positively correlated with 24UP, SCr, BUN, and UA, while it was significantly negatively correlated with eGFR. These results are in accordance with those of Li et al. [35]. In clinical practice, proteinuria and serum creatinine levels are features associated with the progression of IgAN [36]. The above results indirectly suggest that the expression level of miR-320b in urinary exosomes may serve as a novel biomarker for the progression of IgAN.

Nevertheless, the limitations of the present study should be acknowledged. First, the research results are still at an initial stage. The sample size of IgAN included in the study is relatively small, and no independent validation group was established. All analyses were based on the same discovery group, thus the reproducibility and stability of miR-320b could not be verified. Further validation is needed in a larger independent cohort. Second, among the included IgAN patients, no patient demonstrated TA/IF scores > 50%, which might be attributed to routine urine tests and the fact that all the patients selected for renal biopsy were in the early to middle stages. Still, multicenter studies should be conducted to investigate patients with TA/IF scores > 50%. Third, we did not establish a healthy control group or other control groups for kidney diseases, so we were unable to prove whether miR-320b is specifically upregulated in the TA/IF lesions of patients with IgAN. In future studies, we will add healthy control groups or other control groups for kidney diseases to improve this significant deficiency. Finally, due to budgetary constraints, down-regulated miRNAs were not analyzed.

Conclusion

Urinary exosome miRNA expression profiles differ significantly among IgAN patients with varying TA/IF scores. Notably, significantly higher miR-320b levels are observed in patients with high TA/IF scores compared to those with low scores. Additionally, urinary exosome miR-320b promotes EMT in HK-2 cells, highlighting its potential as a non-invasive biomarker for predicting TA/IF scores in IgAN. Future work will focus on identifying the target genes of miR-320b and elucidating the mechanisms of renal fibrosis progression in IgAN to identify effective targets.

Acknowledgements

The authors extend their heartfelt thanks to their families for their understanding and support during the research and writing process. This study was supported by the Zhejiang Medical and Health Science and Technology Program (No. 2025KY1729) and the Zhejiang Traditional Chinese Medicine Science and Technology Project (No. 2025ZX283).

Written informed consent was obtained from all the participants prior to the enrollment of this study.

Disclosure of conflict of interest

None.

Address correspondence to: Jiahua Jin, Department of Ultrasound, Shaoxing Second Hospital, Shaoxing 312000, Zhejiang, China. Tel: +86-15925803800; E-mail: sxjjh0825@163.com

References

[1] Li L, Gong Z, Xue P, Wang D, Xu M, Sui S and Li L. Expression of miRNA-223 and NLRP3 gene in IgA patients and intervention of traditional Chinese medicine. Saudi J Biol Sci 2020; 27: 1521-1526.

[2] Chen T, Xia E, Chen T, Zeng C, Liang S, Xu F, Qin Y, Li X, Zhang Y, Liang D, Xie G and Liu Z. Identification and external validation of IgA nephropathy patients benefiting from immunosuppression therapy. EBioMedicine 2020; 52: 102657.

[3] Gan Y, Li J, Wu J, Zhang R, Han Q, Li Z and Yang Q. Association between geriatric nutritional risk index and pathological phenotypes of IgA nephropathy. PeerJ 2023; 11: e14791.

[4] Liu L, Duan A, Guo Q, Sun G, Cui W, Lu X, Yu H and Luo P. Detection of microRNA-33a-5p in serum, urine and renal tissue of patients with IgA nephropathy. Exp Ther Med 2021; 21: 205.

[5] Liu Y, Wang F, Zhang Y, Jia J and Yan T. ST6GaI1 is up-regulated and associated with aberrant IgA1 glycosylation in IgA nephropathy: an integrated analysis of the transcriptome. J Cell Mol Med 2020; 24: 10493-10500.

[6] Wan Q, Zhou J, Wu Y, Shi L, Liu W, Ou J and Gao J. TNF-alpha-mediated podocyte injury via the apoptotic death receptor pathway in a mouse model of IgA nephropathy. Ren Fail 2022; 44: 1216-1226.

[7] Shen Y, Zhu Z, Wang R, Yan L, Sun S, Lu L, Ren Z and Zhang Q. Chemokine (C-C motif) receptor 2 is associated with the pathological grade and inflammatory response in IgAN children. BMC Nephrol 2022; 23: 215.

[8] Zhang K, Tang L, Jiang SS, Wang YF, Meng Y, Wang MD, Cui FQ, Cai Z and Zhao WJ. Is hyperuricemia an independent prognostic factor for IgA nephropathy: a systematic review and meta-analysis of observational cohort studies. Ren Fail 2022; 44: 70-80.

[9] Liang P, Li S, Yuan G, He K, Li A, Hu D, Li Z and Xu C. Noninvasive assessment of clinical and pathological characteristics of patients with IgA nephropathy by diffusion kurtosis imaging. Insights Imaging 2022; 13: 18.

[10] Thery C, Zitvogel L and Amigorena S. Exosomes: composition, biogenesis and function. Nat Rev Immunol 2002; 2: 569-579.

[11] Valadi H, Ekstrom K, Bossios A, Sjostrand M, Lee JJ and Lotvall JO. Exosome-mediated transfer of mRNAs and microRNAs is a novel mechanism of genetic exchange between cells. Nat Cell Biol 2007; 9: 654-659.

[12] Tosar JP, Witwer K and Cayota A. Revisiting extracellular RNA release, processing, and function. Trends Biochem Sci 2021; 46: 438-445.

[13] Fenton RA. Proteomic approaches in kidney disease biomarker discovery. Am J Physiol Renal Physiol 2018; 315: F1817-F1821.

[14] Chau BN, Xin C, Hartner J, Ren S, Castano AP, Linn G, Li J, Tran PT, Kaimal V, Huang X, Chang AN, Li S, Kalra A, Grafals M, Portilla D, Mackenna DA, Orkin SH and Duffield JS. MicroRNA-21 promotes fibrosis of the kidney by silencing metabolic pathways. Sci Transl Med 2012; 4: 118r-121r.

[15] Li Y, Yu H, Ma Q, Wei M, Liu X, Qi Y, Li C, Dong L and Zhang H. Si-PDGFRbeta-loaded exosomes suppress the progression of glioma by inhibiting the oxidative associated PI3K/Akt/EZH2 signaling pathway. Oxid Med Cell Longev 2022; 2022: 5081439.

[16] Yu Y, Bai F, Qin N, Liu W, Sun Q, Zhou Y and Yang J. Non-proximal renal tubule-derived urinary exosomal miR-200b as a biomarker of renal fibrosis. Nephron 2018; 139: 269-282.

[17] Wang Y, Liu Y, Zhang L, Bai L, Chen S, Wu H, Sun L and Wang X. MiR-30b-5p modulate renal epithelial-mesenchymal transition in diabetic nephropathy by directly targeting SNAI1. Biochem Biophys Res Commun 2021; 535: 12-18.

[18] Lv QL, Du H, Liu YL, Huang YT, Wang GH, Zhang X, Chen SH and Zhou HH. Low expression of microRNA-320b correlates with tumorigenesis and unfavorable prognosis in glioma. Oncol Rep 2017; 38: 959-966.

[19] Zhou J, Zhang M, Huang Y, Feng L, Chen H, Hu Y, Chen H, Zhang K, Zheng L and Zheng S. MicroRNA-320b promotes colorectal cancer proliferation and invasion by competing with its homologous microRNA-320a. Cancer Lett 2015; 356: 669-675.

[20] Bronisz A, Godlewski J, Wallace JA, Merchant AS, Nowicki MO, Mathsyaraja H, Srinivasan R, Trimboli AJ, Martin CK, Li F, Yu L, Fernandez SA, Pecot T, Rosol TJ, Cory S, Hallett M, Park M, Piper MG, Marsh CB, Yee LD, Jimenez RE, Nuovo G, Lawler SE, Chiocca EA, Leone G and Ostrowski MC. Reprogramming of the tumour microenvironment by stromal PTEN-regulated miR-320. Nat Cell Biol 2011; 14: 159-167.

[21] Luo M, Deng S, Han T, Ou Y and Hu Y. LncRNA NR2F2-AS1 functions as a tumor suppressor in gastric cancer through targeting miR-320b/PDCD4 pathway. Histol Histopathol 2022; 37: 575-585.

[22] Yan S, Wang T, Huang S, Di Y, Huang Y, Liu X, Luo Z, Han W and An B. Differential expression of microRNAs in plasma of patients with prediabetes and newly diagnosed type 2 diabetes. Acta Diabetol 2016; 53: 693-702.

[23] Wang H, Cao F, Li X, Miao H, E J, Xing J and Fu CG. MiR-320b suppresses cell proliferation by

targeting c-Myc in human colorectal cancer cells. BMC Cancer 2015; 15: 748.
[24] Song QH, Guo MJ, Zheng JS, Zheng XH, Ye ZH and Wei P. Study on targeting relationship between miR-320b and FGD5-AS1 and its effect on biological function of osteosarcoma cells. Cancer Manag Res 2020; 12: 13589-13598.
[25] Tan N, Tang J, Chen G, Jiang W and Liu Z. ZEB1-AS1 mediates bone metastasis through targeting miR-320b/BMPR1A axis in lung cancer. Clin Respir J 2024; 18: e13770.
[26] Li Q, Zhang B, Lu J, Wa Q, He M, Xie L and Zhang L. SNHG1 functions as a ceRNA in hypertrophic scar fibroblast proliferation and apoptosis through miR-320b/CTNNB1 axis. Arch Dermatol Res 2023; 315: 1593-1601.
[27] Liu T, Li P, Li J, Qi Q, Sun Z, Shi S, Xie Y, Liu S, Wang Y, Du L and Wang C. Exosomal and intracellular miR-320b promotes lymphatic metastasis in esophageal squamous cell carcinoma. Mol Ther Oncolytics 2021; 23: 163-180.
[28] Lee HH, Lee AJ, Park WS, Lee J, Park J, Park B, Joung JY, Lee KH, Hong D and Kim SH. Epithelial splicing regulatory protein (ESPR1) expression in an unfavorable prognostic factor in prostate cancer patients. Front Oncol 2020; 10: 556650.
[29] Wang Y, Shi M, Yang N, Zhou X and Xu L. GPR115 contributes to lung adenocarcinoma metastasis associated with LAMC2 and predicts a poor prognosis. Front Oncol 2020; 10: 577530.
[30] Liu XN, Wang S, Yang Q, Wang YJ, Chen DX and Zhu XX. ESC reverses epithelial mesenchymal transition induced by transforming growth factor-beta via inhibition of Smad signal pathway in HepG2 liver cancer cells. Cancer Cell Int 2015; 15: 114.
[31] Kim Y and Ghil S. Regulators of G-protein signaling, RGS2 and RGS4, inhibit protease-activated receptor 4-mediated signaling by forming a complex with the receptor and Galpha in live cells. Cell Commun Signal 2020; 18: 86.
[32] Kazantseva J, Sadam H, Neuman T and Palm K. Targeted alternative splicing of TAF4: a new strategy for cell reprogramming. Sci Rep 2016; 6: 30852.
[33] Dong GW, Do NY and Lim SC. Relation between proinflammatory mediators and epithelial-mesenchymal transition in head and neck squamous cell carcinoma. Exp Ther Med 2010; 1: 885-891.
[34] Liang Z, Tang S, He R, Luo W, Qin S and Jiang H. The effect and mechanism of miR-30e-5p targeting SNAI1 to regulate epithelial-mesenchymal transition on pancreatic cancer. Bioengineered 2022; 13: 8013-8028.
[35] Li S, Hao H, Li R and Guo S. Urinary exosomal MicroRNAs as new noninvasive biomarkers of IgA nephropathy. Tohoku J Exp Med 2022; 256: 215-223.
[36] Zhang Y and Man L. Albumin-to-fibrinogen ratio is an independent predictor of corticosteroid response and prognosis in patients with IgA nephropathy. Eur J Med Res 2023; 28: 146.

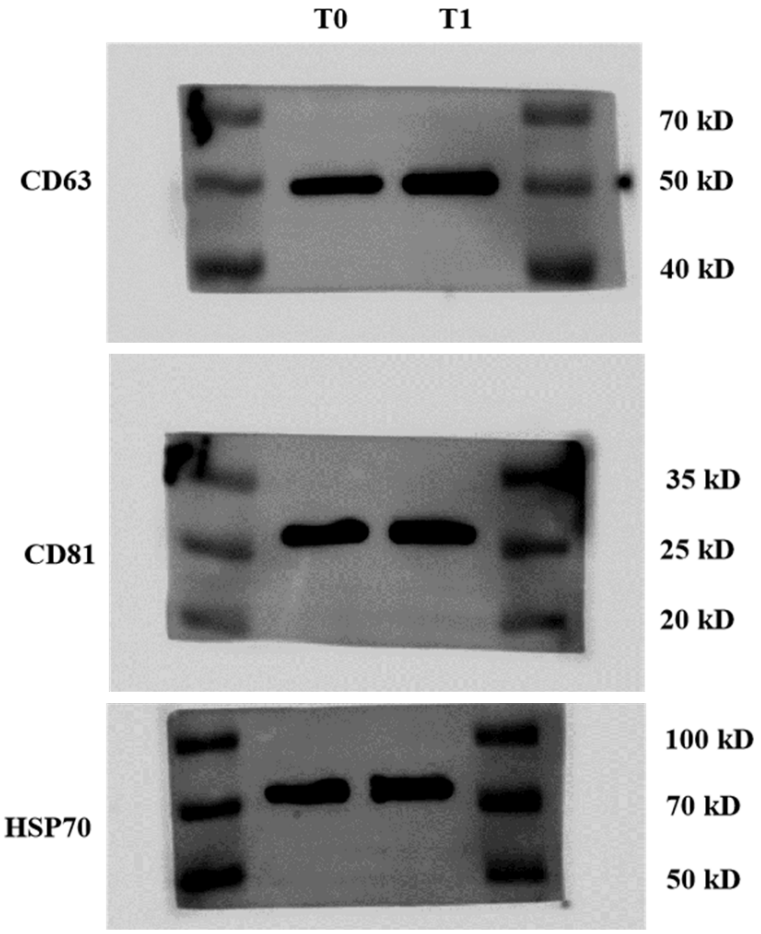

Supplementary Figure 1. Western blotting analysis of exosome biomarkers (CD63, CD81, HSP70).